RESISTIVITY IN CARBONATES: NEW INSIGHTS

M. Fleury
Institut Français du Pétrole

ABSTRACT

A detailed explanation of the non-Archie behavior of the resistivity index vs Sw curves in carbonates is proposed. The model is based on resistivity index (RI) curves measured at ambient and reservoir conditions, on double or triple porosity micritic and oolitic carbonates. We used the Fast Resistivity Index Measurement (FRIM) method to obtain accurate and continuous RI curves down to very low water saturation (5%). In general, the measured RI curves cannot be described by an Archie's law and the measurements at very low saturation are often a key observation to confirm a non-Archie behavior. A large variety of shapes is observed and the local saturation exponents can vary from 1 up to 3.

These shapes can be explained qualitatively and quantitatively using two new models (DPC and TPC) in which the different porosity systems are connected together either in series or in parallel, or a combination of both. The second key feature of the models is the use of NMR and mercury injection curves to estimate the pore volume fraction of each population and the sequence of invasion of each population by oil during the primary drainage process. Hence, only two of three adjustable parameters are needed to model the experimental results. In particular, the saturation exponent of the dominant pore system can be extracted from the analysis. For field applications, we also propose a simple procedure to calibrate resistivity logs with variable saturation exponent.

From the experimental results and the model, we conclude that the pore structure plays a key role. In particular, the microporosity can be responsible for the low resistivity contrast in carbonates, although it may represent less than 10 % of the total pore volume. The water contained in the microporosity forms a continuous path for the current. When invaded by oil, the conductivity of the microporosity system is weakly modified.

INTRODUCTION

Carbonate reservoir evaluation is a challenging task for petrophysicists and a fine understanding of transport properties in these porous media is still lacking. Relative to siliclastics, carbonates may be simpler in terms of mineralogy but are incomparably more complex in terms of pore structure and surface properties. A large biological origin of the sediments combined with various diagenetic processes yield complex pore structure, which may differ greatly from one reservoir to another. In many carbonate systems, resistivity laboratory calibrations contradict field observations (water-free production, capillary pressure) as well as direct water saturation measurements from preserved cores.

In carbonates, the understanding and prediction of the effect of pore structure combined with those of wettability on the electrical properties is a real scientific challenge, both theoretically

and experimentally. It has a major impact on the estimation of oil in place, especially for the giant oil fields of the Middle East, because the deviation from standard values (e.g. m and n of 2) is so large that water saturation estimation can vary over more than 20%. A good review of the various experimental observations can be found in Sen [1], who also proposes theoretical explanations based on the existence of distinct pore populations (micro, macro and mesopores) mixed in various ways. In general, the resistivity index curve RI(Sw), where RI=Rt/Ro is the resistivity of the rock at a water saturation Sw divided by the resistivity at Sw=1, cannot be described by a power law (second Archie's law $RI=Sw^{-n}$) and n is a function of saturation itself. The problems are concentrated in the RI curves because the validity of the first Archie's law for obtaining Ro as a function of porosity appears to be much less problematic and not as sensitive to pore structure. Petricola and Watfa [2] suggest that the microporosity may act as a parallel path for the current yielding decreasing n values and therefore, to a gradual insensitivity of the resistivity to saturation, as observed in shaly sands. Dixon and Marek [3] also suggest that the microporosity is responsible for the low n values measured (typically 1.45), but n did not depend on the saturation itself in the saturation range considered. At the opposite, Bouvier et al. [4] observed that n can increase greatly in certain conditions and suggest a link of the RI(Sw) curve with the capillary pressure curve. Increasing n values is also a well-known effect of wettability which tends to favor the discontinuity of the water phase and therefore increase the resistivity compared to the water-wet case. The wettability effect can lead either to an abrupt increase of n or to a high value of n without discontinuity [5]. Therefore, a confusion is possible.

From the works mentioned above and from our own (unpublished) observations, a tentative sketch of the various shapes of the RI(Sw) curves is shown in Figure 1. Four shapes can be distinguished:

- Type I: may be typical of carbonates from the Thamama formation ([2] and this study),
- Type II: bending up at intermediate saturation [4], flattening at low saturation (this study),
- Type III: single slope at low saturation, extrapolation to Sw=1 above Ir=1 (this study),
- Type IV: typical of oil wet systems, large n values sometimes increasing further at low saturation. This is also valid in clastics.

The purpose of this paper is an attempt to explain at least qualitatively the various shapes already observed, except type IV which will be treated separately in future works. For example, a parallel model has been cited in the literature but never developed in details to extract the electrical properties of each network. A key aspect in these new insights is the availability of a powerful experimental technique to measure a continuous resistivity index curve instead of the traditional technique giving a limited number of points at capillary equilibrium.

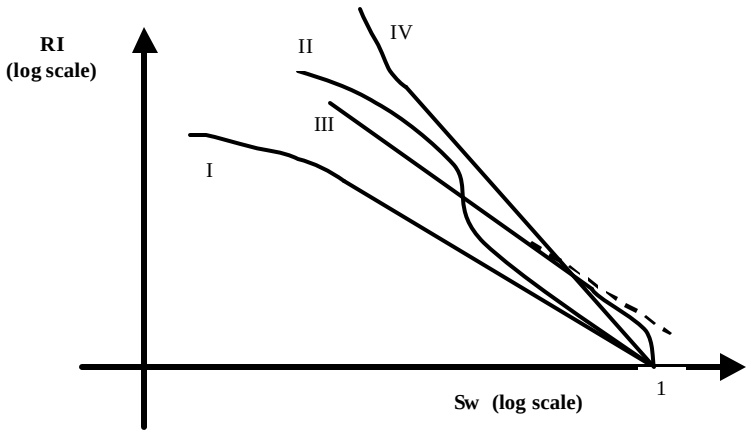

Figure 1: Schematic of the different types of RI curves observed experimentally. I to III are due to the pore structure, IV is typical of wettability effects and is not specific to carbonates.

EXPERIMENTS

Samples

We present the measurements performed on three selected carbonate samples having double or triple porosity systems (permeability and porosity are listed in Table 1). The first one is a reservoir carbonate sample from the Middle East classified as a packstone. It has been cleaned with various solvents at elevated temperature before the measurements. At ambient conditions, the experiment has been performed with refined oil and synthetic reservoir brine. The reservoir condition experiment has been performed with filtered dead crude oil at the reservoir temperature. After cleaning, the sample's wettability is moderately water wet and after aging, it is strongly oil wet. The other two samples are (water wet) outcrop carbonates. The porosity of the Brauvillier limestone (BL) is essentially intergranular and due to the oolithe's cortex. The porosity of the Estaillade limestone is both inter and intragranular.

All these samples are characterized by a bi or trimodal pore size distribution as indicated by NMR relaxometry. The pore populations are separated by at least a factor of 10. It is worth recalling the notion of pore in relation with NMR relaxometry. When detected by low field NMR, a pore class gathers all the pores with identical surface to volume ratio (S/V) that are not coupled by diffusion to neighboring pores during measuring time. Although it is difficult to calibrate precisely T_2 relaxation times into pore sizes, T_2 values below 10 ms are characteristic times of micropores in the usual sense [6].

Table 1: Sample properties. Water salinity: 30 gr/l NaCl for EL and BL, 150 gr/l for RC.

Sample	Type	Porosity (%)	Permeability (mD)
Reservoir carbonate (RC)	Packstone	15	0.1
Estaillade limestone (EL)	Biosparite grainstone	29.5	124
Brauvillier limestone (BL)	Oobiosparite grainstone	30	14

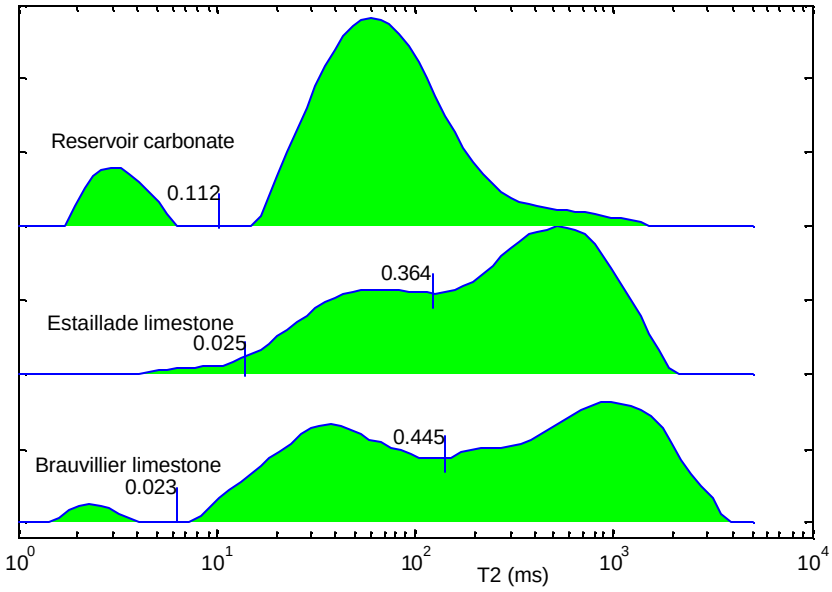

Figure 2: NMR pore size distribution of the 3 carbonates studied. The numbers indicate the pore volume fraction at the left of the vertical segment.

Resistivity Index Measurements

The Fast Resistivity Index Measurement (FRIM) method has been used to perform the measurements. This method is discussed extensively in [7] and [8]. We highlight here the important aspects of the method and present the latest improvements.

In the FRIM method, we perform a pressure imposed oil-water displacement on a plug of length 2.5 cm and diameter 4 cm. It is very similar to a 'Porous Plate' displacement process except that capillary equilibrium is not needed. At ambient conditions, only 2 or 3 pressure steps are used. At reservoir conditions using dead or live oil, the experiment should not be conducted too rapidly, that is no faster than needed for the stabilization of wettability to occur at a given saturation. Therefore, the drainage is performed in about 2 to 3 weeks which is the typical kinetic of chemical processes involved in aging [9]. The simplicity of the method lies in the fact that only the average saturation and resistance need to be recorded and plotted in real time to obtain a continuous resistivity index curve free of artifacts. The key point is that the radial electrode geometry allows to investigate the entire sample volume and to compensate for the non-uniform saturation profile occurring in the absence of capillary equilibrium.

At ambient conditions, we used the CAPRIWET cell as described in [8] in a frequency range 50 mHz-10 MHz (only the measurements of the real part of the impedance at 1 kHz are presented in this paper). At reservoir conditions, we used a standard set-up where the

confining sleeve has been modified. The complex impedance measurements are performed at a fixed frequency of 1 kHz and the real part extracted to compute resistivity index. The highest capillary pressure imposed is 10 Bar (for an interfacial tension γ =35 mN/m; at reservoir conditions with crude oil, the maximum capillary pressure is reduced proportionally to the interfacial tension).

CONDUCTIVITY MODELS

Double Porosity Conductivity (DPC) Model

The objective is to explain RI curves bending down at low saturation (type I in Figure 1). The double porosity model envisioned here is essentially very close to those proposed for shaly sandstones where the clays present at the surface of the pores act as a parallel path for the current. For carbonates, we assume the existence of two pore networks acting electrically in parallel. This is essentially the way to reproduce a curve flattening at (very) low saturation. The main two ingredients in our model are the description of the invasion of the pore network during drainage, and the description of the electrical arrangement of the two different pore populations.

The first network 1 (e.g. macropores) represents most of the pore volume while the second network 2 (micropores) represents only a small fraction not necessarily above percolation thresholds. First, we consider the saturation of each network Sw_1 and Sw_2 that are linked to the measured average saturation Sw according to:

$$Sw = f_1 Sw_1 + f_2 Sw_2 \text{ where } f_1 + f_2 = 1 \quad (1)$$

f_1 and f_2 are the pore volume fraction of each population. These fractions can be evaluated using NMR relaxometry. Second, we assume that the networks are invaded by oil at different capillary pressures; the small pores are accessed at a higher pressure than the large pores. From the capillary pressure curve, this pressure corresponds to an average saturation Sc that can be inferred from mercury injection curves (indicating pore throat size distribution). We can express Sw_1 as a function of Sw at high Sw:

$$Sw_1 = \frac{Sw + f_1 - 1}{f_1}, \quad Sw_2 = 1 \quad \text{for} \quad Sw \geq Sc \quad (2)$$

Below Sc, the relationships Sw_1=f(Sw) and Sw_2=f(Sw) need further assumptions. We will assume (i) a linear relationship and (ii) that $Sw_1 \rightarrow 0$, $Sw_2 \rightarrow 0$ when $Sw \rightarrow 0$. We deduce:

$$Sw_1 = \frac{f_1 + Sc - 1}{f_1 Sc} Sw, \quad Sw_2 = \frac{Sw}{Sc} \quad \text{for} \quad Sw \leq Sc \quad (3)$$

We consider now the conductivity of each network. When initially saturated with brine, the total conductivity Ct_0 for the two networks in parallel will be:

$$Ct_0 = C_1 + C_2 = C_1(1 + a) \text{ where } C_2 = a \ C_1 \quad (4)$$

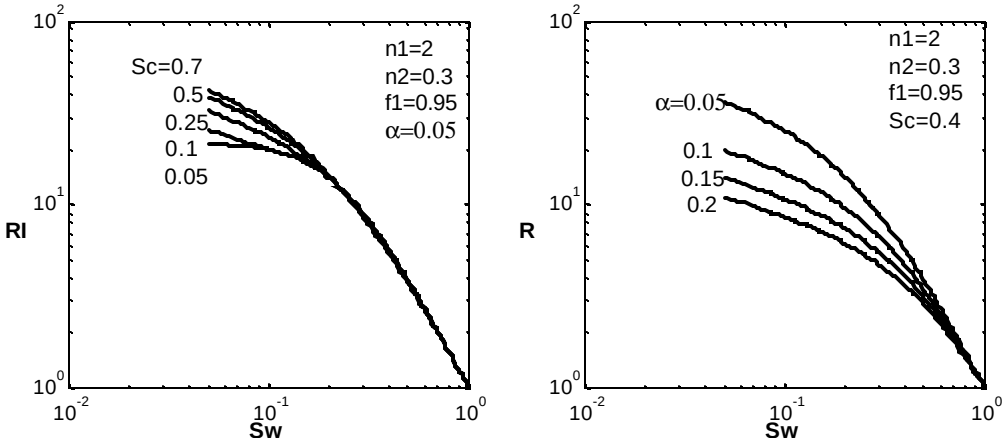

Figure 3: Sensitivity of the DPC model to the saturation Sc at which the microporosity is invaded by oil (left), and to α, the initial conductivity ratio of the two pore populations.

The parameter α is the conductivity ratio of the two networks saturated at 100%. From the first Archie's law, we expect C_1 and C_2 to be related to the pore volume fraction of each population and therefore, α is expected to be of the order of the ratio f_2/f_1. When the two networks are invaded by oil, we assume that each conductivity is linked to saturation through a power law (as in the second Archie's law). The total conductivity in the two saturation domains is:

$$Ct = Sw_1^{n1} C_1 + C_2 \quad \text{for} \quad Sw \geq Sc \tag{5}$$

$$Ct = Sw_1^{n1} C_1 + Sw_2^{n2} C_2 \ \text{for} \ Sw \leq Sc \tag{6}$$

Using Eq. 4, the resistivity index RI is:

$$RI = \frac{Ct_0}{Ct} = Sw_1^{-n1} \frac{1+a}{1+a \ \ Sw_1^{-n1}} \ \text{for} \ Sw \geq Sc \tag{7}$$

$$RI = Sw_1^{-n1} \frac{1+a}{1+a \ \ Sw_1^{-n1} / Sw_2^{-n2}} \ \text{for} \ Sw \leq Sc \tag{8}$$

When one pore population dominates (network 1 in the present case), the RI functions are governed by the resistivity properties (n_1) of this population. Eq. 7 and Eq. 8 are essentially similar to the formulas used in shaly sandstones except that we introduce a second exponent n_2 characterizing the second network.

In the DPC model, there is a total of 4 parameters n_1, n_2, α and Sc. For a given experimental curve, Sc is measured separately with some degree of uncertainty, while the other parameters are fitted. There is however a range of variation of α around f_2/f_1 for which

there is a physical meaning. At high Sw, the slope in log-log scale of RI(Sw) is $-n_1$, and at low saturation, the slope is $-n_2$. To some degree, Sc and α are compensating each other (Figure 3), but α is the most sensitive parameter controlling the final RI value. Note that the case Sc=0.05 in Figure 3 corresponds to the situation where the second network is not invaded by oil, yielding a horizontal asymptote.

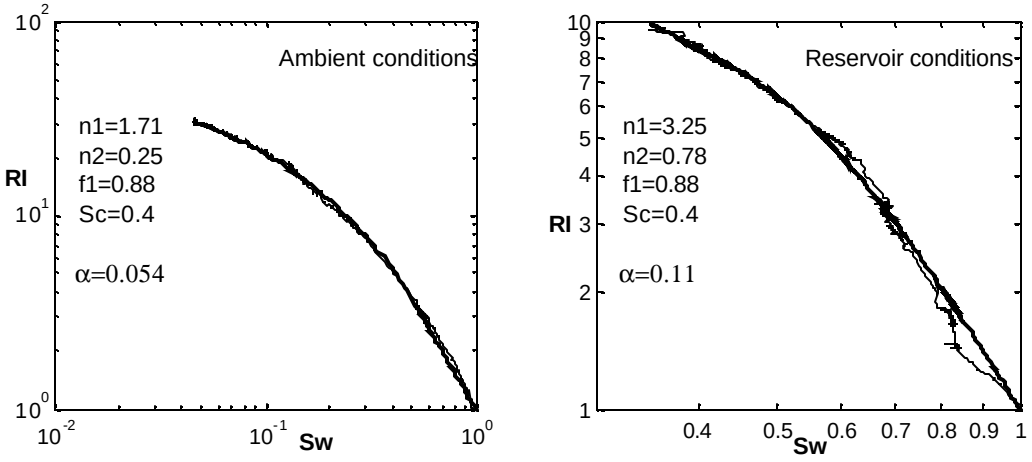

Figure 4: Application of the DPC model on sample RC at ambient (left) and reservoir temperature using dead oil (right). Experimental curve (thin line) and model (thick line). The parameters n_1, n_2 and α are fitted, f_1 and Sc are measured.

The parameters of the model were adjusted to fit the experimental RI curve measured on sample RC. The value of Sc=0.4 was deduced from the kink on the mercury injection capillary pressure curve and the pore volume fraction f_1=0.88 of macropores (network 1) was deduced from NMR (Figure 2). Despite the low permeability of the sample, the lowest saturation obtained is very small (4%), allowing a good determination of the model's parameter at ambient conditions. The initial slope of the RI curve is n_1=1.71 and characterizes network 1. Network 2 is very weakly sensitive to saturation (n_2=0.25) and does not behave as a standard network. However, the initial conductivity ratio α=0.054 of network 1 to 2 is of the order of magnitude of f_2/f_1= 0.136. At reservoir conditions (oil wet conditions), there is a strong increase of n_1 but the RI curve is still not linear in log-log scale. The characteristics n_2=0.78 and α=0.11 of the second network are also slightly modified but the accuracy on these parameters is weaker than at ambient condition because the saturation reached (at the same capillary pressure) is much higher and close to Sc.

Triple Porosity Conductivity (TPC) Model

The objective is to explain RI curves bending up at intermediate or high saturation and down at low saturation in log-log scale, (type II and III in Figure 1). We use here the general idea that complex carbonates can have three populations of pores labeled for simplicity micro,

macro and mesopores (respectively 3, 2 and 1). As in the double porosity model, we consider the saturation of the 3 populations:

$$Sw = f_1 Sw_1 + f_2 Sw_2 + f_3 Sw_3 \text{ where } f_1 + f_2 + f_3 = 1 \quad (9)$$

Again, the invasion by oil during drainage of these populations is assumed to be sequential. If the network 1 is invaded first, we define an average saturation Sm at which the network 2 is invaded:

$$Sw_1 = \frac{Sw - f_2 - f_3}{f_1} \text{ , } Sw_2 = 1 \quad Sw_3 = 1 \text{for} \quad Sw \geq Sm \quad (10)$$

Below Sm, many scenarios can be imagined. In general we will assume linear relationships for the functions $Sw_1(Sw)$ and $Sw_2(Sw)$. As a possible scenario, we will assume $Sw_1 \rightarrow 0$, $Sw_2 \rightarrow 0$ when $Sw \rightarrow Sc$. Sc is the saturation at which the microporosity is invaded. It follows:

$$Sw_1 = \frac{Sw - f_2 Sw_2 - f_3}{f_1} \text{ , } Sw_2 = \frac{Sw - Sc}{Sm - Sc} \text{ , } Sw_3 = 1 \text{ for } Sc \leq Sw \leq Sm \quad (11)$$

The invasion scenario is summarized in Figure 5. Typically, we have in mind a situation where $f_3 << f_1$ and $f_1 \approx f_2$, and the microporosity (network 3) is invaded at a pressure much too high to be observed in the experiments.

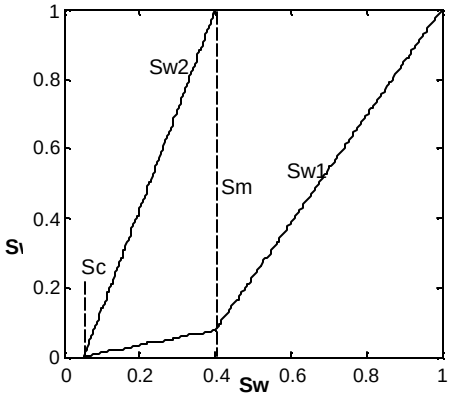

Figure 5: Invasion scenario in the TPC model.

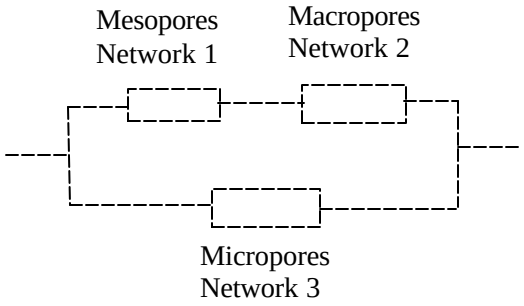

Figure 6: Electrical arrangement of the 3 networks in the triple porosity conductivity (TPC) model.

Let us now consider the conductivity of these populations. We assume that the networks 1 and 2 are in series while the network 3 is in parallel as shown in Figure 6. The arrangement in series may seem in contradiction with a sequential invasion by oil (which is essentially a parallel mechanism) but such a situation is possible. This point is discussed further later. At Sw=1, the conductivity Ct_0 of the system shown in Figure 6 is:

$$Ct_0 = (C_1^{-1} + C_2^{-1})^{-1} + C_3 = C_1 \left[(1 + a_1^{-1})^{-1} + a_2 \right] \text{ where } C_2 = a_1 C_1, C_3 = a_2 C_1 \quad (12)$$

In the two saturation domains, one obtains:

$$Ct = C_1\left[(Sw_1^{-n1} + a_1^{-1})^{-1} + a_2\right] \quad \text{for} \quad Sw \geq Sm \tag{13}$$

$$Ct = C_1\left[(Sw_1^{-n1} + Sw_2^{-n2}a_1^{-1})^{-1} + a_2\right] \quad \text{for} \quad Sc \leq Sw \leq Sm \tag{14}$$

Resistivity index can be calculated from Eq 12 to Eq. 14. For measured values of f_1, f_2 and f_3, one has to adjust n_1, n_2, α_1 and α_2 to the experimental data. In a similar way as in the DPC model, one expects to find α_1 of the order of f_2/f_1 and α_2 of the order of f_3/f_1.

This model was tested with resistivity index curves measured on sample EL and BL. On sample EL (Figure 7), the bending up of the curve at high saturation is reproduced qualitatively at high saturation and the flattening at low saturation is well reproduced. There is a discontinuity at Sm (deduced from the kink in the mercury injection capillary pressure curve) because there is also an abrupt change in the $Sw_1(Sw)$ relationship (such as the one shown in Figure 5). From the fit, the two dominant pore populations have similar characteristics ($n_1=n_2=1.5$). The third population acting as a parallel circuit is not invaded by oil and is only characterized by the conductivity ratio α_2. On the sample BL (Figure 8), the RI curve can be explained by a similar mechanism of resistance in series but with a very high Sm value. We find that the two networks have quite different n values and that network 2 is much less conductive than network 1 ($\alpha_1=7.1$).

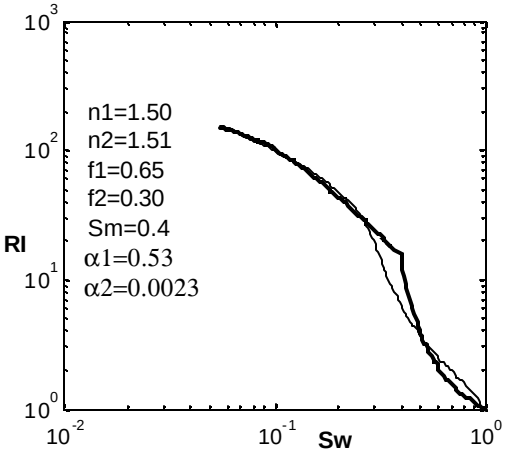

Figure 7 : Measured RI curve (thin line) and model (thick line) for sample EL (Estaillade limestone).

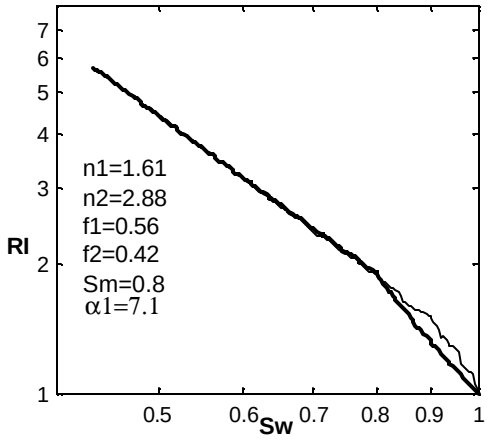

Figure 8 : Measured RI curve (thin line) and model (thick line) for sample BL (Brauviller limestone).

DISCUSSION

In all situations, the proposed models (DPC and TPC) can well reproduce the flattening of RI curves at low saturation which is due to a parallel electrical path. The effect of parallel conductivity is effective already at high saturation and the curve will never be linear in log-log scale. However, when one consider only a limited saturation range (e.g. [0.2 1]), the curve could be approximated by an Archie's law, with an average n value which will be quite small

compared to the reference value of 2. This may explain the low n values found by Dixon and Marek (1990).

The microporosity network does not behave as a classical water wet porous structure with saturation exponent n close to 2. For example, sample RC contains 12% of microporosity while the lowest saturation reached is 4%. Therefore, this pore population must be invaded by oil. The weak sensitivity to saturation (about $Sw^{-0.5}$ or less) suggests that another specific mechanism of conduction must be found for the microporosity (the minerals themselves are assumed to be non-conductive). Note that in shaly sand model, the conductivity of the shales is assumed to vary linearly with Sw.

Assembling two pore populations in series gives the appropriate shape. However, the TPC model does not give a smooth representation of the conductivity at high saturation and this may give inaccurate values of n_1 or n_2. This is partly due to the assumptions concerning the relationships $Sw_1(Sw)$ and $Sw_2(Sw)$ (Eq. 11). These functions could be accessed experimentally by combining simultaneous NMR and capillary pressure experiments. However, the main reason is more likely related to an arrangement where the two dominant populations are also partly in parallel, the series arrangement being dominant. This can be imagined when considering a packing of grains that are themselves porous. These networks are essentially in series. During oil invasion in the intergranular porosity, there is an increase of the resistance of one network but the grain to grain contact will maintain to some degree a parallel path.

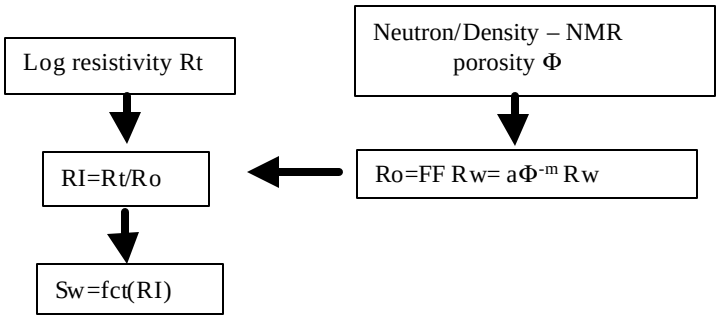

Figure 9 : Simplified calibration sequence for resistivity logs. For non-Archie type rocks, the Sw(RI) is needed. Laboratory data usually provide the RI(Sw) relationship.

LOG CALIBRATION APPLICATION

When Archie's laws are valid, the saturation is deduced from the measured log resistivity Rt using the sequence indicated in Figure 9. While the first Archie's law is very robust and verified for a large variety of rocks (m may need however to be determined for a given rock type), the use of the second Archie's law with a variable n depending on saturation is not convenient. What is needed in fact is the inverse relationship Sw(Ir) which is not easily

deduced from the model. We suggest first an approximate formula reducing Eq. 7 and Eq. 8 into one single formula valid for type I curves. First we note that:

$$Sw_2^{n2} Sw_1^{-n1} \approx Sc^{-n2} Sw^{n2-n1} \approx Sw^{n2-n1} \quad \text{with} \quad Sw_1 \cong Sw \text{ and } Sc^{-n2} \approx 1 \qquad (15)$$

providing $f_2 << f_1$. Applying Eq. 8 in the entire saturation range yields:

$$RI = Sw^{-n1} \frac{1+C}{1+CSw^{n2-n1}} \qquad (16)$$

As seen in Figure 10, the use of the 3 parameters n_1, n_2 and C are sufficient to describe accurately the data using 16. Here, the meaning of C is approximately the same as α and may depend on temperature. The formulation given in Eq. 16 can be used to describe standard experiments performed at capillary equilibrium in which a limited number of points is available. However, despite this simplification, the inverse relationship Sw-Ir is still difficult to extract. As a very general method, we suggest to use a polynomial fit in log-log scale :

$$\log(\mathrm{Sw}) = \sum_{i=1}^{4} A_i \log(\mathrm{RI})^i \qquad (17)$$

Using a 4th order polynomial, an accurate description of the data is obtained (Figure 10). This type of equation can easily be implemented in interpretation softwares to accurately deduce water saturation from deep resistivity logs.

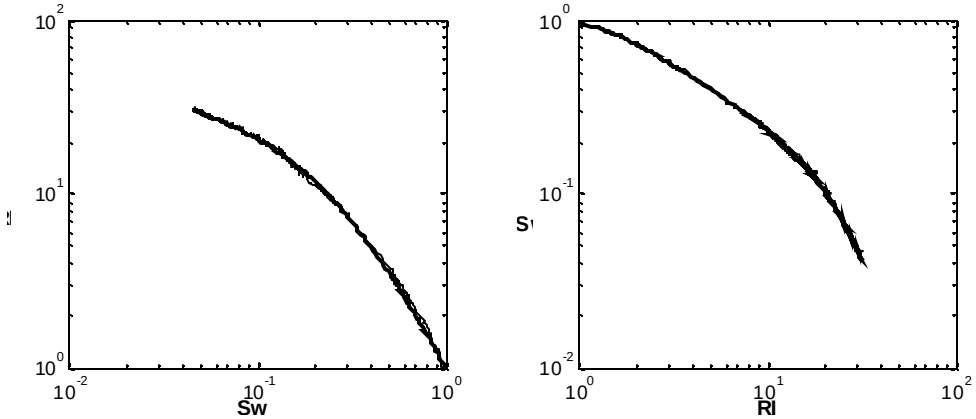

Figure 10 : Log calibration procedure example on sample RC. Left: the experimental RI(Sw) curve is fitted with equation 16. Right: using the same data, the inverse relationship Sw(RI) is fitted with equation 17 and can be used directly in log calibration procedure.

CONCLUSION

The non-Archie behavior of some carbonate rocks can be explained by a parallel or series arrangement of the pore populations. In double porosity systems (DPC model), the mechanism to obtain a flattening of the RI curves at low saturation is a parallel path generated by the microporosity. In triple porosity systems (TPC model), the mechanism to

obtain a bending up of the RI curves is a series arrangement of the two dominant pore populations, while the microporosity stays always in parallel.

When a continuous RI curve is available, the parameters characterizing the different populations can be identified. The number of parameters to adjust is also kept to a minimum by using simple measurements such as mercury injection capillary pressure curves and NMR relaxation time distribution.

ACKNOWLEDGEMENT

We acknowledge ADCO and its management for permission to use one freshly preserved reservoir core sample and fluids. We thank also D. Longeron and L. Cuiec for their constructive comments.

REFERENCES

1. Sen P.N., Resistivity of partially saturated carbonate rocks with microporosity, Geophysics, Vol. 62, NO. 2, P. 415-425, 1997.
2. Petricola M.J.C. and M. Watfa, Effect of microporosity in carbonates: introduction of a versatile saturation equation, Soc. Petr. Eng. 29841, SPE Middle Eastern Oil Show, Bahrain, 607-615, 1995.
3. Dixon J.R. and B.F. Marek, The effect of bimodal pore size distribution on electrical properties of some middle eastern limestone , Soc. Petr. Eng. 20601, 7th SPE Middle Eastern Oil Show, Bahrain, 743-750, 1990.
4. Bouvier L. and S.M. Maquignon, "Reconciliation of log and laboratory derived irreducible water saturation in a double porosity reservoir", Advances in Core Evaluation, edited by P.F. Worthington and D. Longeron, Gordon and Breach Science Publishers, 1991.
5. Longeron D., D.G. Argaud and L. Bouvier, 'Resistivity index and capillary pressure measurements under reservoir conditions using crude oil', Soc. Petr. Eng. 19589, 64th annaul Tech. Conf. , 1989.
6. Moore C.H., Carbonate reservoirs, Porosity evolution and diagenesis in a sequence stratigraphic framework, Developments in sedimentology 55, Elsevier Ed., 2001.
7. Fleury M., 1998, "FRIM: a Fast Resistivity Index Measurement Method", Proceeding of the International Symposium of the Society of Core Analysts, Den Hague,14-16 September 1998.
8. Fleury M. and F. Liu, Frequency effect on resistivity index curves using a new method, Proceedings of the 41st Annual SPWLA Symposium, Dallas, June 4-7 2000.
9. Cuiec L.E., 'Evaluation of reservoir wettability and its effect on oil recovery', Interfacial Phenomena in Oil Recovery, N.R. Morrow (ed), Marcell Dekker, New York, 1990.